Theoretical and Experimental Thermal Performance Analysis of Building Shell Components Containing Blown Fiberglass Insulation Enhanced with Phase-Change Material (PCM)

Jan Kosny, PhD
Member ASHRAE

David Yarbrough, PhD
Member ASHRAE

Phil Childs

Som Shrestha, PhD
Member ASHRAE

William Miller, PhD
Member ASHRAE

Jerry Atchley

Marcus Bianchi, PhD
Member ASHRAE

John Smith
Associate Member ASHRAE

Tom Fellinger
Associate Member ASHRAE

Elizabeth Kossecka, PhD

Edwin Lee
Student Member ASHRAE

ABSTRACT

Different types of phase-change materials (PCMs) have been tested as dynamic components in buildings during the last four decades. Most historical studies have found that PCMs enhance building energy performance. Some PCM-enhanced building materials, like PCM-gypsum boards or PCM-impregnated concretes, have already found limited applications in different countries. Today, continued improvements in building envelope technologies suggest that throughout southern and central US climates, residences may soon be routinely constructed with PCM in order to maximize insulation effectiveness and maintain low heating and cooling loads. This paper presents experimental and numerical results from thermal performance studies. These studies focus on blown fiberglass insulation modified with a novel spray-applied microencapsulated PCM. Experimental results are reported for both laboratory-scale and full-sized building elements tested in the field. In order to confirm theoretical predictions, PCM-enhanced fiberglass insulation was evaluated in a guarded hot-box facility to demonstrate heat flow reductions when one side of a test wall is subjected to a temperature increase. The laboratory work showed reductions in heat flow of 30% due to the presence of approximately 20 wt % PCM in the insulation. Field testing of residential attics insulated with blown fiberglass and PCM was completed in Oak Ridge, Tennessee. Experimental work was followed by detailed whole building EnergyPlus simulations in order to generate energy performance data for different US climates. In addition, a series of numerical simulations and field experiments demonstrated a potential for application of a novel PCM fiberglass insulation as enabling technology to be used during the attic thermal renovations.

TECHNICAL BACKGROUND

During the late 1980s and early 1990s, Oak Ridge National Laboratory (ORNL) tested several configurations of gypsum boards enhanced with phase-change materials (PCMs) (Tomlinson et al. 1992). In 1994, blends of lightweight aggregates and salt hydrates were analyzed and tested (Petrie et al. 1997), and in 2002, an ORNL research team started working on fiber insulations blended with microencapsulated PCMs (Kosny et al. 2006, 2007a, 2007b). These PCM–insulation mixtures function as lightweight thermal mass components. It is expected that these types of dynamic insulation systems will contribute to the objective of reducing energy use in buildings and to the development of "zero-net-

Jan Kosny *was a senior research scientist at Oak Ridge National Laboratory (ORNL), Oak Ridge, TN, and is currently at the Fraunhofer Center for Sustainable Energy Systems, CSE, Cambridge, MA.* ***David Yarbrough*** *was a senior research scientist and is currently in R&D services at ORNL.* ***William Miller*** *is a senior research scientist and* ***Som Shrestha*** *and* ***Phil Childs*** *are research engineers at ORNL.* ***Jerry Atchley*** *is with the Building Envelopes Group, ORNL.* ***Marcus Bianchi*** *was a R&D staff member at Johns Manville Technical Center, Littleton, CO, and is currently a senior research scientist at National Renewable Energy Laboratory, Golden, CO.* ***John Smith*** *and* ***Tom Fellinger*** *are R&D staff members at Johns Manville.* ***Elizabeth Kossecka*** *is head of the Department of Eco-Building Engineering at the Polish Academy of Sciences, Warsaw, Poland.* ***Edwin Lee*** *is a doctoral student at Oklahoma State University, Stillwater, OK.*

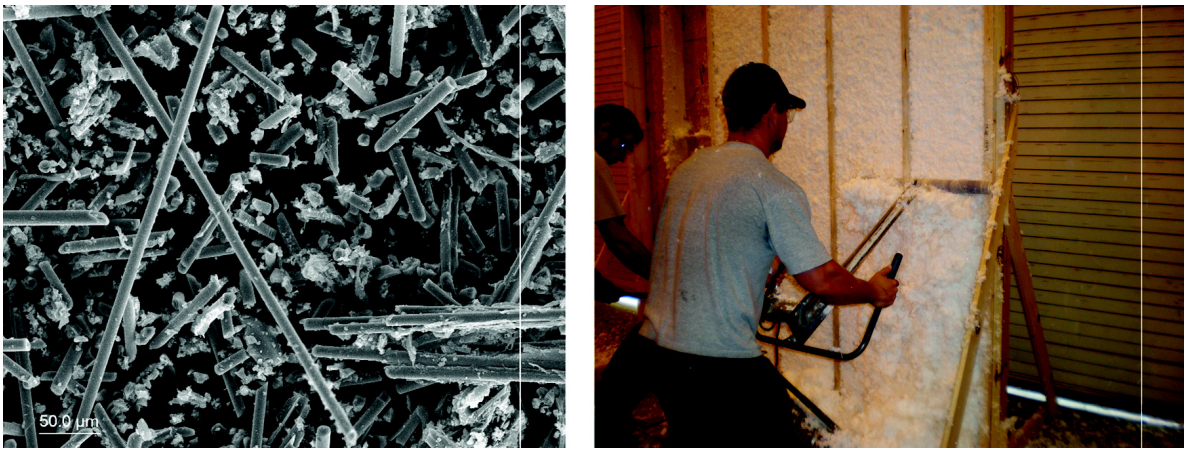

Figure 1 *Microscopic view of a complex network of glass fibers within the blown insulation, and installation of the blown fiberglass into the test wall.*

energy" buildings. This is a consequence of this technology's ability to reduce energy consumption for space conditioning and reshape peak-hour loads. Other anticipated advantages of PCMs include improvements in occupant comfort, compatibility with traditional wood and steel framing technologies, and potential for application in retrofit projects.

ORNL research demonstrated that PCMs can be mixed with fiber insulations, incorporated into structural and sheathing materials, or packaged for localized application. Results from a series of small-scale laboratory measurements and field experiments indicate that a new generation of PCM-enhanced fiber insulations could have excellent potential for successful application in US buildings because of their ability to reduce energy consumption for space conditioning and reduce peak loads (Kosny 2008; Kosny et al. 2009). New PCM applications require a careful selection of materials, identification of PCM locations, bounding of thermal resistances, and specification of the amount of PCM to be used. This paper describes the results from small-scale dynamic testing, laboratory-scale testing, and full-size field testing of building elements using PCM-enhanced blown fiberglass insulation.

The major goal of this work was experimental and numerical analysis of the energy performance of PCM-enhanced fiberglass insulation with relatively complex, multilayer configuration of two or more different materials, including blown glass fibers (Figure 1), very fine PCM powders, adhesives, and the occasional use of fire retardants. The amount of PCM in the insulation blend must be accurately determined before any further thermal analysis can be performed. This is not a trivial task (Kosny et al. 2009). During the installation process, specific amounts of PCM are added to the fibrous insulation in multilayer fashion. For the purpose of this project, a 20% blend of PCM and proprietary adhesive blend was used. This new material was jointly used with blown fiberglass, as shown on Figure 1.

THERMAL BALANCE OF A ONE-DIMENSIONAL SAMPLE OF PCM-ENHANCED THERMAL INSULATION

The estimated area heat storage capacity for a specific PCM-enhanced product is a key indicator of its future dynamic thermal performance. A theoretical model of the material with temperature-dependent specific heat can be used to calculate phase-change processes in most common materials (Kossecka and Kosny 2009). The one-dimensional heat transport equation for such a case is

$$\frac{\partial}{\partial t}(\rho h) = \frac{\partial}{\partial x}\left[\lambda \frac{\partial T}{\partial x}\right], \tag{1}$$

where ρ and λ are the material density and thermal conductivity, and h and T are enthalpy density and temperature.

The enthalpy derivative over the temperature (with consideration of constant pressure) represents the effective heat capacity, with phase-change energy being one of the components:

$$c_{eff} = \frac{\partial h}{\partial T}. \tag{2}$$

After Equation 1 is integrated over the thickness d and time interval $[t_1, t_2]$, we can obtain the thermal balance of the equation associated with the enthalpy change generated by heat transfer between the top and bottom surfaces of the sample. After changing the integration order, and assuming constant material density, we obtain

$$\int_{t_1}^{t_2}\int_{0}^{d} \frac{\partial}{\partial t}(\rho h)\,dx\,dt = \int_{0}^{d} \rho\,\Delta h(x, t_1, t_2)\,dx = \int_{t_1}^{t_2} [q(0) - q(d)]\,dt \tag{3}$$

$$q(x, t) = -\lambda \frac{\partial T(x, t)}{\partial x} \tag{4}$$

where q is heat flux.

The increase of enthalpy density Δh at point x and in time interval $[t_1, t_2]$ is caused by the temperature change. It can be expressed as follows:

$$\Delta h(x, t_1, t_2) = \int_{t_1}^{t_2} \frac{\partial h}{\partial t} dt = \int_{t_1}^{t_2} \frac{\partial h}{\partial T} \frac{\partial T}{\partial t} dt = \int_{T(x,t_1)}^{T(x,t_2)} c_{eff}(x, T) dT \quad (5)$$

Integration of $c_{eff}(x, T)$ over temperature can be conducted in the case in which the final temperature distribution in the sample is known. However, in specific cases, such as the addition of uniformly distributed PCM to thermal insulation, it is possible to determine enthalpy change without performing detailed heat transfer calculations. The change can be expressed as

$$c_{eff} = (1 - \alpha) c_{ins} + \alpha c_{effMicr}, \quad (6)$$

where α denotes the percentage of PCM, c_{ins} denotes the specific heat of insulation without PCM, and $c_{effMicr}$ denotes the effective heat capacity of microencapsulated PCM.

In this project, a new type of non-petroleum-based PCM was used. This product received the 2009 R&D 100 award. The project team combined the following elements to produce a sturdy, efficient, flame-resistant product:

- A microencapsulated PCM having a methyl ester core, which is less costly and less flammable than paraffin
- Smaller particles (3–6 μm, reduced from a typical size of ~15 μm)
- A flame retardant applied to the capsule surfaces during drying
- A flame-retardant additive applied to produce 30–50 μm aggregates
- A design in which the PCM is not directly exposed to the interior of the building

The addition of low levels of various inorganic flame retardants to the exterior of the capsules provides an added layer of ignition resilience protection.

The phase change enthalpy of this new organic PCM is about 170 J/g (73 Btu/lb), which is an approximate 40% improvement when compared to the competitive paraffinic PCMs. Figure 2 depicts the temperature-dependent enthalpy change for microencapsulated PCM, generated by differential scanning calorimeter (DSC) testing. In this material, the phase-change process takes place at 29°C (84°F). The effective heat capacity of PCM may be represented by a specific heat equation denoted by:

$$c_{effMicr}(T) = c_l + (c_{effMicr}(T) - c_l), \quad (7)$$

where c_l represents the specific heat in the liquid state, which is constant for PCM.

The integral over the temperature range of the phase change process represents the melting total enthalpy density H_m. It can be denoted by Equation 8:

$$\int_{T_1}^{T_2} (c_{effMicr}(T) - c_l) dT = H_m \quad (8)$$

Now, let us assume, for a sample of material containing PCM, an asymptotic heating process from initial steady-state conditions characterized by boundary temperatures on both surfaces of T_{01} and T_{d1}, to another steady-state condition with a higher boundary temperature of ΔT. Let us also assume that the initial temperatures T_{01} and T_{d1} are below the freezing point of the PCM, and that heating by ΔT will melt all of the PCM. After performing integration on Equation 5 with an assumption of constant thermal density and thermal conductivity, and taking into account Equations 6, 7, and 8, the heat balance Equation 3 will look as follows:

$$\int_{t_1}^{t_2} [q(0) - q(d)] dt = \rho d \{ c_{ins} \Delta T + \alpha [(c_l - c_{ins}) \Delta T + H_m] \} \quad (9)$$

Equation 9 can be used for an experimental determination of the amount of PCM in blends with other materials if all the thermal characteristics of all the other individual components of these blends are known. In this case, the transient heat flow meter apparatus experiment can be used. Detailed testing procedure was presented by Kosny et al. (2009) during the 2009 Effstock Conference in Stockholm, Sweden. In earlier works (Kossecka 1998; Kossecka and Kosny 2002, 2008), similar testing was used for determination of thermal characteristics of PCMs necessary for numerical energy analysis.

ENCOURAGING RESULTS OF DYNAMIC HOT-BOX MEASUREMENTS OF A WALL CONTAINING PCM-ENHANCED FIBERGLASS INSULATION

Since 1998, ORNL has been the world's only laboratory performing dynamic hot-box experiments on a daily bases. In this project, an 8ft × 8 ft wood-framed wall containing blown fiberglass insulation combined with microencapsulated PCM was used for dynamic hot-box testing. The test wall was constructed with nominal 2 in. × 6 in. studs installed on 16 in. spacing. As shown on Figure 1, three wall cavities were insulated with conventional blown fiberglass at a density of about 29 kg/m^3 (1.8 lb/ft^3). The other three wall cavities were insulated with a multilayered fiberglass-PCM mixture.

As shown in Figure 3, the test wall cavity was instrumented with temperature sensors installed at 2.5 cm (1 in.) intervals. The first 2/3 of the wall thickness (counting from the interior surface) was filled with conventional blown fiberglass of the same density as in the other non-PCM section of the wall. The remaining part of the wall cavity was filled with several layers of proprietary PCM blend with adhesive and blown fiberglass. The test wall contained approximately

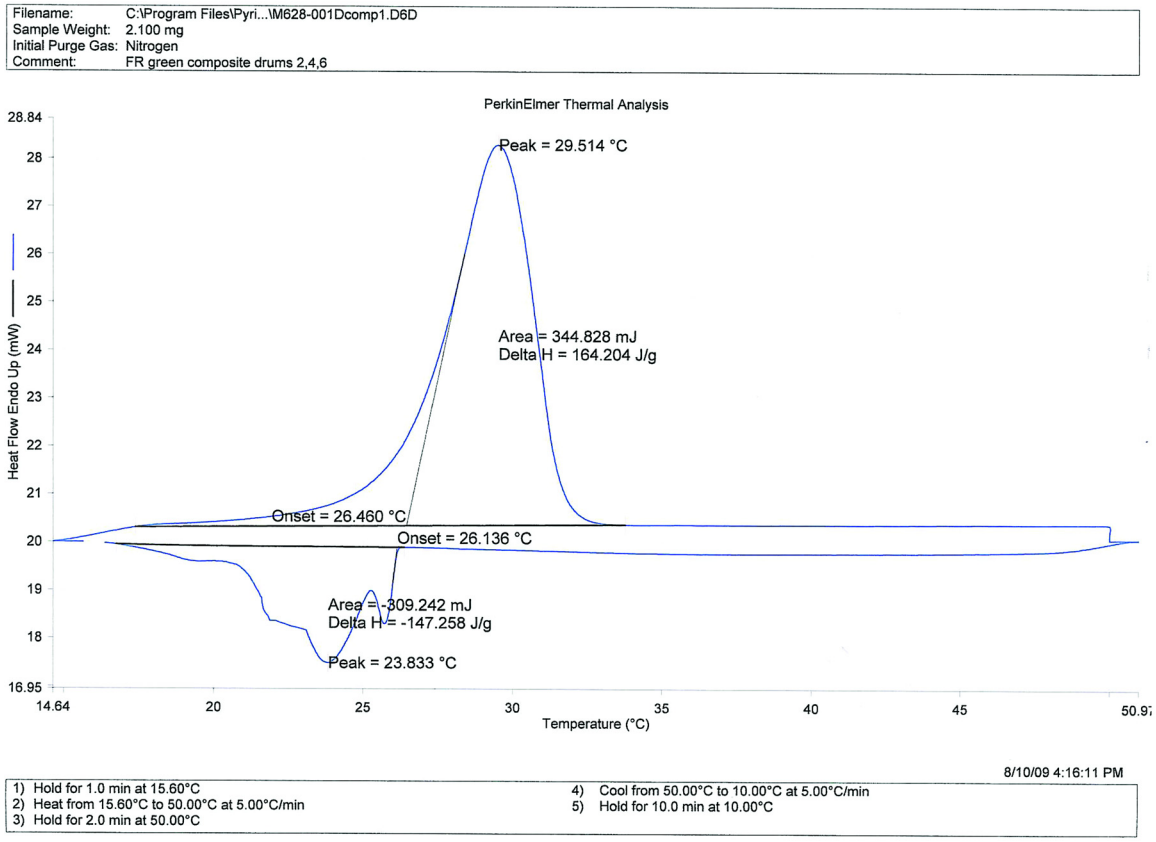

Figure 2 *Temperature-dependent enthalpy change for non-petroleum-based microencapsulated PCM used in the project.*

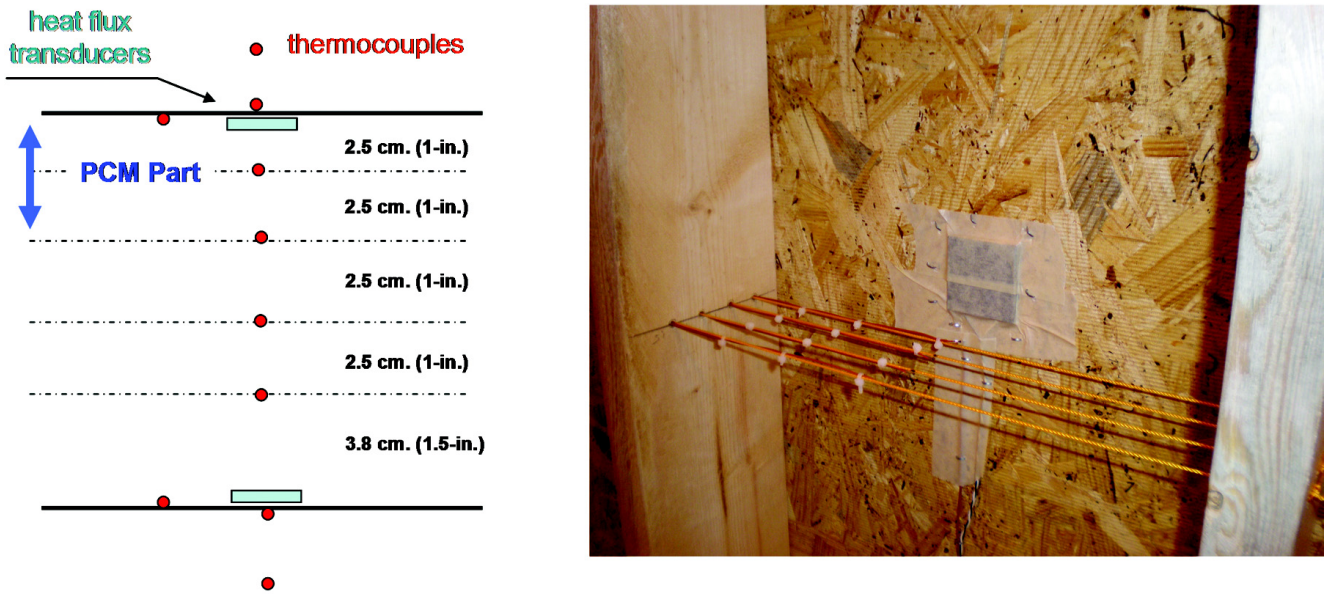

Figure 3 *Schematic of cross section and instrumentation location in the wall specimen used for dynamic hot-box testing of the PCM-enhanced fiberglass insulation.*

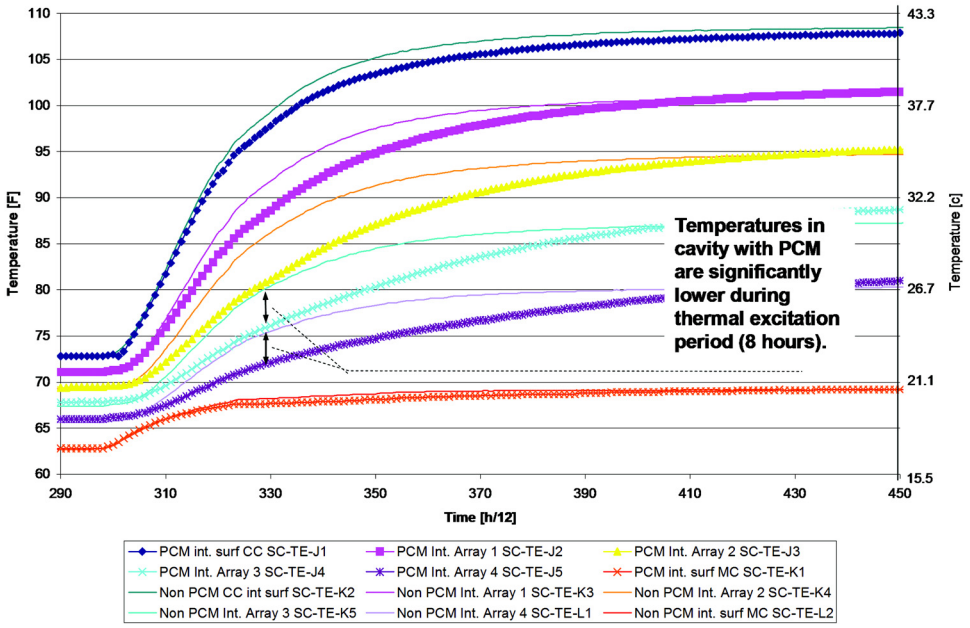

Figure 4 *Temperature profiles recorded during dynamic thermal excitation (thick lines represent PCM section of the wall; thin lines represent non-PCM insulation). "PCM" means PCM part of the wall; "Non PCM" indicates non-PCM insulation; "Array 1,2,3,4" means thermistor distanced 1 in., 2 in., 3 in., or 4 in. from exterior wall cavity surface.*

20 wt.% PCM. It is estimated that about 13.6 kg (30 lb) of PCM-enhanced fiberglass insulation (containing 0.79 kg/m^3 [0.16 lb/ft^2] of PCM) was used for this dynamic experiment. As shown in Figure 2, the PCM melting temperature was about 29°C (84°F). The phase change enthalpy was about 170 J/g (73 Btu/lb).

The dynamic hot-box experiment was performed using the same testing procedure as in earlier tests with use of PCM-impregnated foams and blends of blown cellulose insulation with microencapsulated PCM (Kosny 2008). At the beginning of the measurement, temperatures were stabilized at about 18.3°C (65°F) on the cold side and 22.2°C (72°F) on the warm side. Next, the temperature of the warm side (i.e., the side of the wall cavity containing PCM) was rapidly increased to 43.3°C (110°F). Figure 4 shows temperature profiles recorded in both non-PCM and PCM sections of the test wall during thermal excitation. It can be observed that PCM content in the wall thermally stabilizes the PCM section of the wall. It is associated with significantly lower local temperatures in the wall part containing PCM during the rapid heating process. Thermal lag time for that heating process is between 7 to 8 hours for the PCM part of the wall.

Test-generated heat flux results are shown in Figure 5 for both sides of the wall. It took about 8 1/2 hours to fully charge the PCM material within the wall. Heat fluxes on both sides of the wall were measured and compared. For 2 hour and 8 1/2 hour time intervals, heat fluxes were integrated for each surface. Comparisons of measured heat flow rates on the wall surface opposite the thermal excitation enabled estimation of the potential thermal load reduction generated by the PCM. On average, the PCM part of the wall demonstrated over 27% of the cooling effect (total reduction of the heat flow) during 8 1/2 hours, and over 50% during the first 2 hours of the rapid heating process.

In real field conditions, most thermal excitations generated by the climate generally last less than 5 hours (peak hour time). As a comparison, during similar previously conducted hot-box experiments with dynamic cellulose insulation containing uniformly distributed 25% PCM-cellulose blend (Kosny 2008), it was determined that, during the first 5 hours after the thermal ramp period, PCM-enhanced cellulose material reduced the total heat flow through the wall by over 40%. In this case, it took about 15 hours to fully charge walls PCM. Recorded load reductions for the entire 15 hours were close to 20%.

FULL-SCALE FIELD TESTING OF RESIDENTIAL ATTIC CONTAINING PCM-ENHANCED BLOWN FIBERGLASS INSULATION

During July 2008, a full-scale experimental attic was constructed and instrumented in order to field test blown fiberglass insulation combined with microencapsulated PCM. Since melting temperature of organic PCMs can be modified, the main goal of this experiment was to investigate at what level and how often PCM was going through the phase-change process. Collected experimental results are expected to be used for future changes in the attic design, and for eventual optimization of PCM thermal characteristics. As shown in

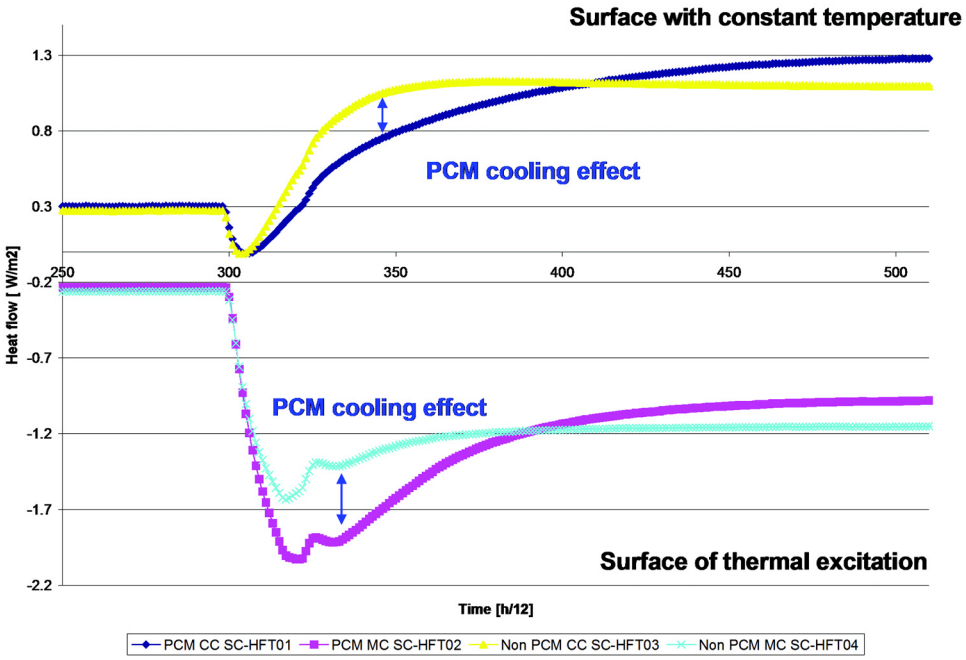

Figure 5 *Heat fluxes recorded during the dynamic hot-box measurement."PCM" means PCM part of the wall; "Non PCM" is non-PCM insulation; "cc" indicates climate side; "mc" means meter side of the hot-box.*

Figure 6, a full-scale residential attic was filled with about 25 cm (10 in.) of blown fiberglass insulation of approximate density 29 kg/m^3 (1.8 lb/ft^3). On top of this insulation, four 1.3 cm (1/2 in.) thick layers of PCM-adhesive blend were installed, with 1.3 cm (1/2 in.) layers of blown fiberglass in between. The total thickness of added PCM-fiberglass multi-layer sandwich was approximately 10 cm (4 in.). PCM melting temperature was at about at 29°C (84°F). As shown in Figure 2, the PCM sub-cooling effect was about 6°C (11°F), with freezing temperature close to 23°C (73°F). The phase-change enthalpy was about 170 J/g (73 Btu/lb).

In this field experiment, a relatively advanced attic containing an over-the-deck ventilated cavity and low-e metal cool roof (solar reflectance SR28, emissivity E81) was used. Monitored test data included the temperatures of the roof deck on both sides of the 5/8 in. oriented strand board (OSB) and the heat flux transmitted through the roof deck. As shown on Figure 7, all test roof decks had a 2 in.^{2} by 0.18 in. deep routed slot with a heat flux transducer (HFT) inserted to measure heat flow crossing the deck. Each HFT was placed in a guard made of the same OSB material used in construction and was calibrated using a FOX 670 heat flow meter to correct for shunting effects (i.e., distortion due to three-dimensional heat flow) (Miller and Kosny 2007). There was a 4 in. ventilated air space between the roof deck and the roof metal cover. Reflective insulation was installed on the top of the roof deck. The attic cavities also had an instrumented area in the floor (i.e., ceiling) for measuring heat flows into the conditioned space. The attic floor under the blown fiberglass insulation consisted of a metal

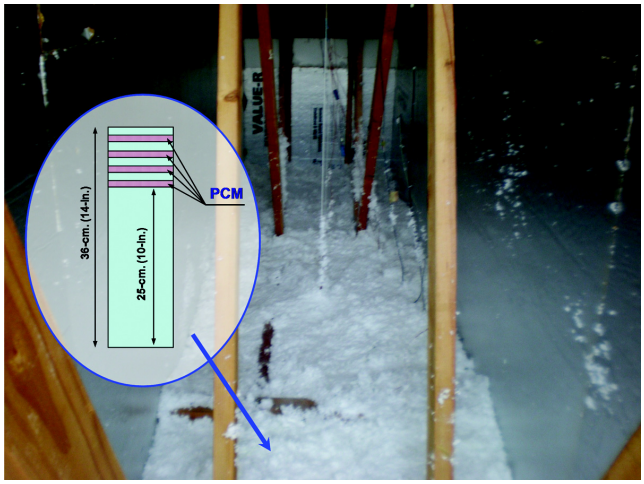

Figure 6 *Photograph of the test attic with blown PCM-enhanced fiberglass insulation.*

deck, a 1 in. thick piece of wood fiberboard lying on the metal deck, and a 1/2 in. thick piece of wood fiberboard placed atop the 1 in. thick piece (Figure 7). The HFT for measuring ceiling heat flow was embedded between the two pieces of wood fiberboard.

In order to estimate optimum attic air temperatures for PCM (to have it fully melted and later fully frozen), a finite-difference model was developed for the test attic. Attic air

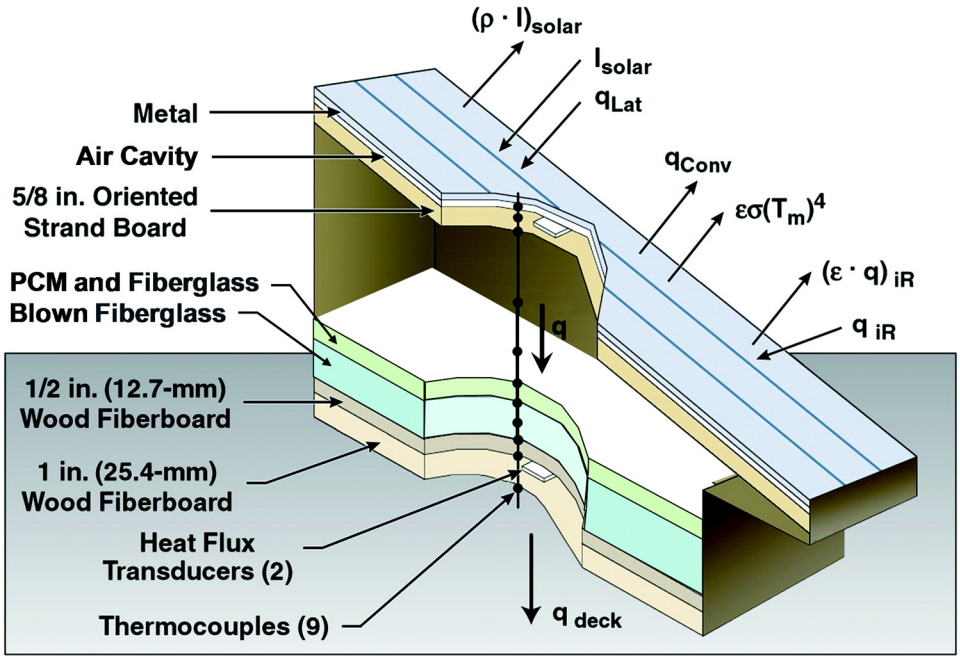

Figure 7 *Schematic of measured temperatures and heat fluxes for test attic with PCM-enhanced blown fiberglass.*

temperatures recorded during the summer of 2006 were used in modeling. Figure 8 depicts simulated temperature profiles within the attic insulation under transient thermal excitations generated by variable attic air temperature. Results of numerical analysis indicated that, in order to make PCM fully melt, attic air temperature during the peak of the day should be higher than 32°C (90°F). During the night, attic air temperature should be below 20°C (68°F).

Detailed temperature profiles across the roof, attic space, and within the attic insulation were collected for two summer seasons in 2008 and 2009. Recorded temperature data for summer months were analyzed from the perspective of optimum conditions for PCM to undergo through full phase changes. It was found that, during the two tested seasons, the second week of May was the beginning week for PCM to start regular freezing and melting. This process ended during the first week of October. An example of recorded temperature profiles for the test attic is presented in Figure 9 for two days (August 17 and 18) in 2008. Characteristic temperature points of melting PCM are as noticeable as in Figure 8 for numerically generated temperature profiles.

As presented in Figure 10, recorded temperature data for summer months were analyzed from the perspective of optimum conditions for PCM to undergo full phase changes. For each month, a number for days when CPM went through a complete phase change process was calculated. It was found that, during the two tested seasons, the second week of May was a beginning week for PCM to have at least two full phase changes a week. This process ended during the first week of October. In May and September, the calculated number of active days for PCM was close to 50% of total number of days. During June and August, on over 75% of days, phase change processes took place. In July, due to increased night temperature, the number of days when PCM was fully active went down to below 50%. In order to improve PCMs' effectiveness during July, a PCM with a higher melting point could be used; however, that approach would reduce the number of active days in May and September. Detailed numerical analysis would be necessary to optimize this design for specific climates.

ANALYSIS OF POTENTIAL USE OF PCM-ENHANCED FIBERGLASS AS ENABLING TECHNOLOGY IN RETROFIT APPLICATIONS

Whole-house energy modeling and full-scale field testing were performed in order to evaluate potential benefits of using PCM-enhanced fiberglass insulation for attic thermal retrofit. At the beginning, a series of EnergyPlus whole-building energy simulations was performed using climatic data for Atlanta and Chicago to analyze the impact of added attic thermal insulation on building energy performance. The building considered for this study was a 16.8 m (55 ft) × 8.4 m (27.5 ft) single-story ranch house with three bedrooms, one living room, and an attic (see Figure 11). The considered task was based on the replacement of existing attic insulation with R_{SI}-6.7 (R-38) blown fiberglass combined with PCM. Three entry levels of existing attic insulation were considered: R_{SI}-2.1 (R-12), R_{SI}-3.3 (R-19), and R_{SI}-5.3 (R-30). It is necessary to mention that a case of the conventional R_{SI}-2.1 (R-12) attic

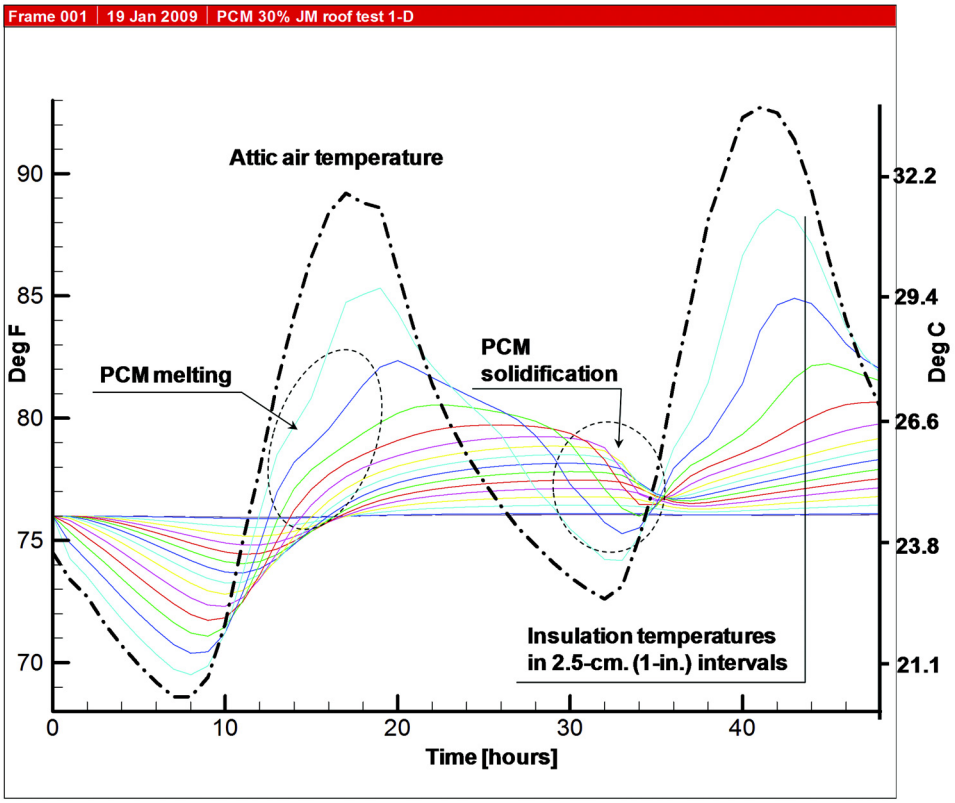

Figure 8 *Simulated temperature profiles within the PCM-enhanced attic insulation under transient thermal excitations.*

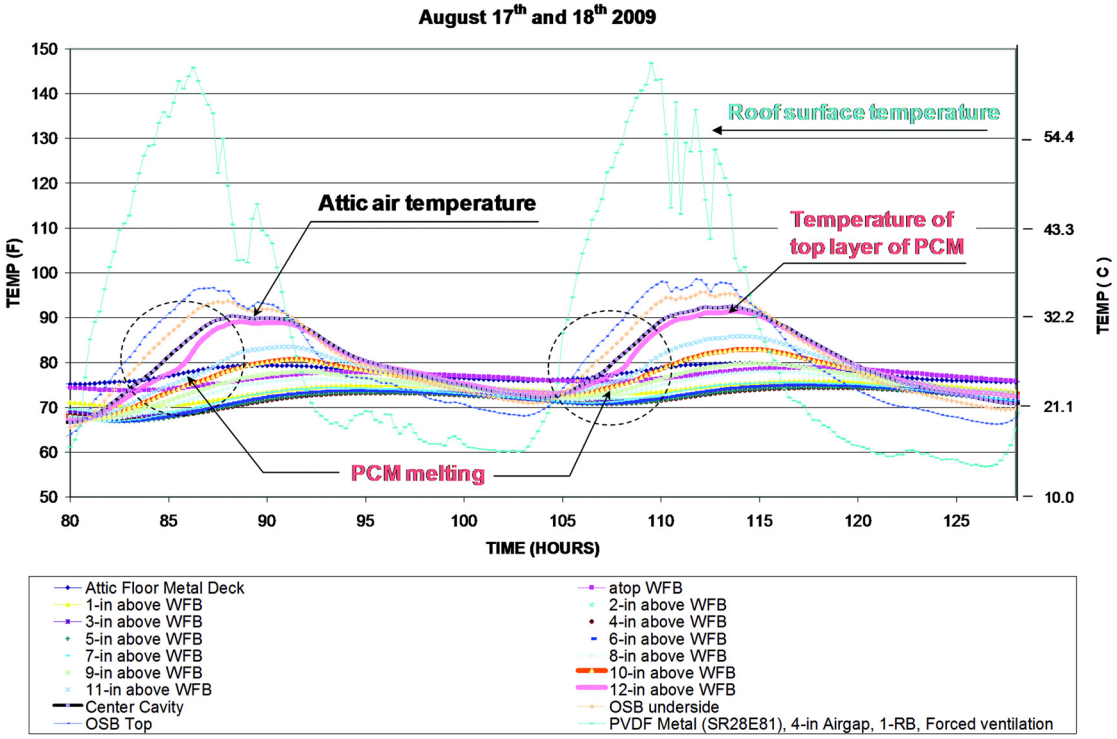

Figure 9 *Test-generated temperature profiles within the experimental attic with PCM-enhanced attic insulation. "WFB" indicates wood fiber board.*

Table 1. Annual Cooling Load Changes due to Improvement of Attic Insulation Computed for Atlanta and Chicago

PCM Addition Attic R-Value Change	Annual Cooling Load Change, %		No PCM Attic R-Value Change	Annual Cooling Load Change, %	
	Atlanta	Chicago		Atlanta	Chicago
R-12 to PCM R-38	10.57%	11.46%	R-12 to R-38	6.81%	7.22%
R-19 to PCM R-38	7.13%	7.79%	R-19 to R-38	3.22%	3.37%
R-30 to PCM R-38	4.84%	5.35%	R-30 to R-38	0.83%	0.81%
R-38 to PCM R-38	4.04%	4.57%			
R-50 to PCM R-38	3.48%	4.16%	R-38 to R-50	0.58%	0.44%

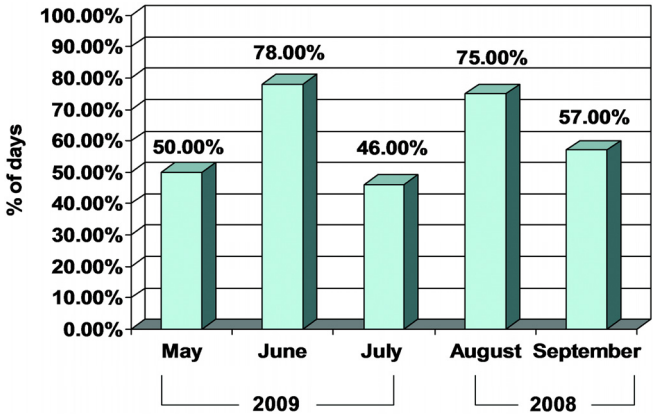

Figure 10 *Recorded percentage of days with PCM undergoing a full phase-change process.*

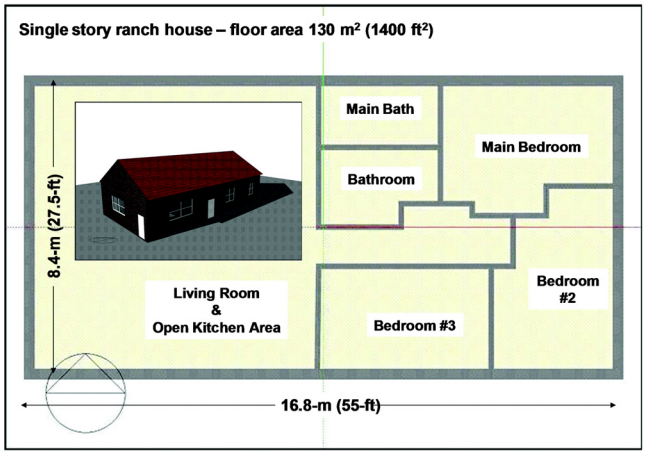

Figure 11 *Floor plan of the one-story ranch house used in whole-house energy simulations.*

represents the approximate effective thermal performance of the most common old residential attic using 14 cm (5.5 in.) fiberglass batts installed with air voids. In addition (in sake of comparison), the two most popular attic levels of insulation were simulated as well: R_{SI}-6.7 (R-38) and R_{SI}-8.8 (R-50).

Attic retrofit work considered in this paper was similar to what was shown on Figures 6 and 7. A full-scale residential attic was filled with about 18 cm (7 in.) of blown fiberglass insulation of approximate density 29 kg/m^3 (1.8 lb/ft^3). Next, on top of this insulation, four 1.3 cm (1/2 in.) thick layers of PCM-adhesive blend were installed with 1.3 cm (1/2 in.) thick layers of blown fiberglass installed in between. The total thickness of the added PCM-fiberglass multilayer sandwich was approximately 10 cm (4 in.). The PCM melting temperature was about 29°C (84°F). The phase-change enthalpy was about 170 J/g (73 Btu/lb). EnergyPlus simulations were performed for both conventional insulation cases and for dynamic insulation containing PCM. Figures 12 and 13 depict total values of ceiling heat flow simulated for two days in July 2008. Five cases of conventional attic insulation were compared against R_{SI}-6.7 (R-38) PCM-enhanced fiberglass. Simulation results for both climates demonstrated a potential for reduction of about 70% to 80% of roof-generated peak-hour loads in the case when conventional R_{SI}-2.1 (R-12) attic insulation was replaced by the R_{SI}-6.7 (R-38) PCM-enhanced fiberglass.

In addition, percentage changes of annual cooling loads were computed for considered levels of attic insulation. Data presented in Table 1 show that thermal retrofitting of the residential attic with PCM-enhanced insulation is significantly more effective than using only conventional insulation. For example, an upgrade from the conventional R_{SI}-2.1 (R-12) insulation to PCM-enhanced R_{SI}-6.7 (R-38) is 1/3 more energy effective than just using conventional insulation of the same R-value. Similarly, an upgrade from the conventional R_{SI}-3.3 (R-19) insulation to PCM-enhanced R_{SI}-6.7 (R-38) improved overall efficiency by more than 50%. Most interesting, the R_{SI}-6.7 (R-38) insulation containing PCM is more efficient than conventional R_{SI}-8.8 (R-50). Because roof thermal loads represent approximately 15% of the total building loads in the considered building, about a 10% change in annual cooling loads represents approximately 65% improvement in scale of the entire roof heat transfer.

During the second part of this project, a full-scale field experiment took place in order to evaluate the potential of using PCM-enhanced fiberglass insulation in attic retrofits.

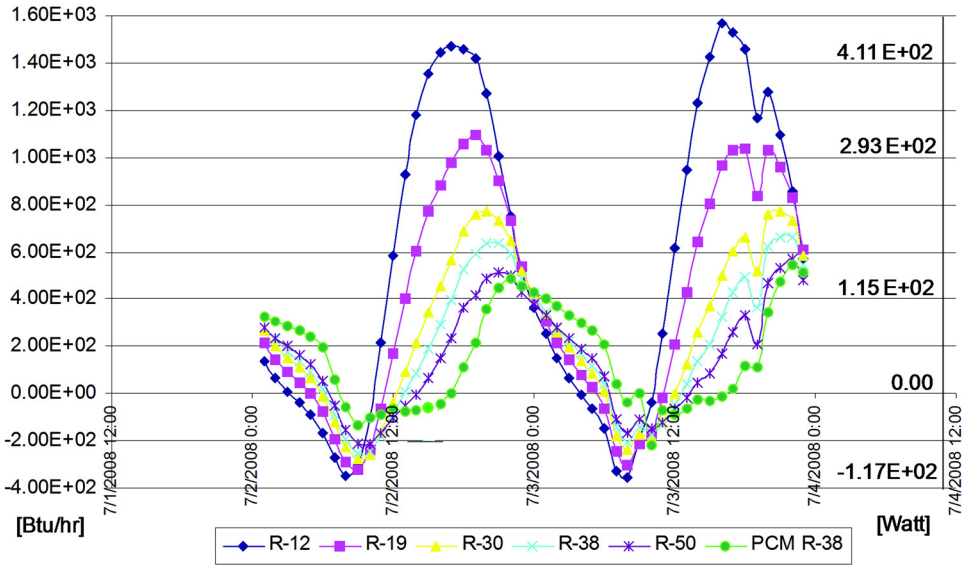

Figure 12 *Comparisons of simulated ceiling heat conduction profiles for Atlanta climatic conditions.*

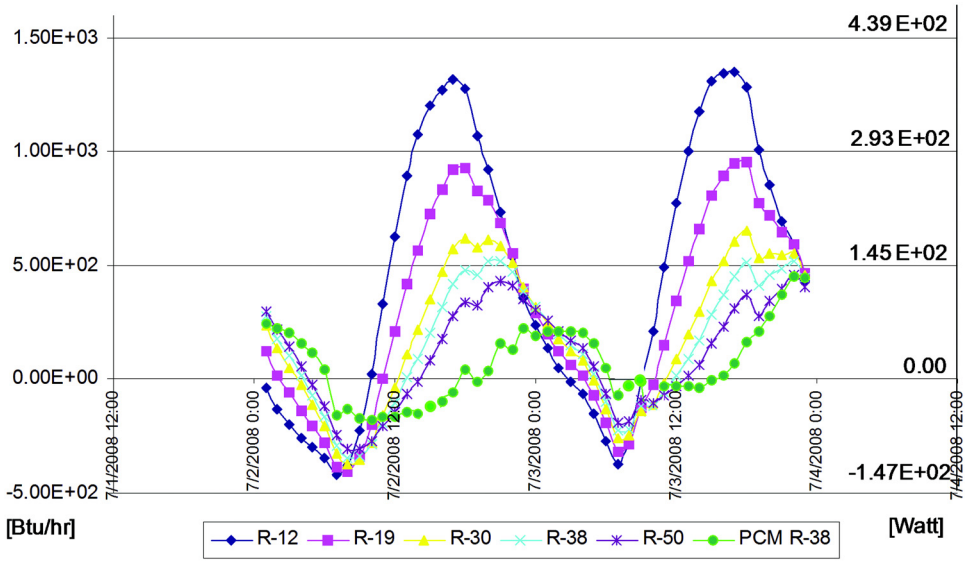

Figure 13 *Comparisons of simulated ceiling heat conduction profiles for Chicago climatic conditions.*

For this purpose, energy performance of poorly insulated attic R_{SI}-1.2 (R-7) with a conventional shingle roof was experimentally compared against the retrofitted attic with advanced roof structure and PCM-enhanced insulations. The question was what level of energy benefits can be achieved in the case of a total reconstruction of poorly insulated existing attic, using state-of-the-art thermal technologies developed during the last decade. The two main goals of this retrofit experiment were to construct a durable roof structure (using a low-labor-intensive process and with roof-over-the-roof construction minimizing solid waste) and significantly reduce summer cooling loads. In order to meet these goals, considered attic reconstruction had five following key elements:

- Roof-over-the-roof installation with metal roof cover
- An application of cool roof coating (SR28 E81)
- Installation of vented air cavity
- Installation of reflective insulation inside the roof air cavity
- Installation of about R_{SI}-8.5 (R-48) of blown fiberglass insulation with the top layer containing PCM

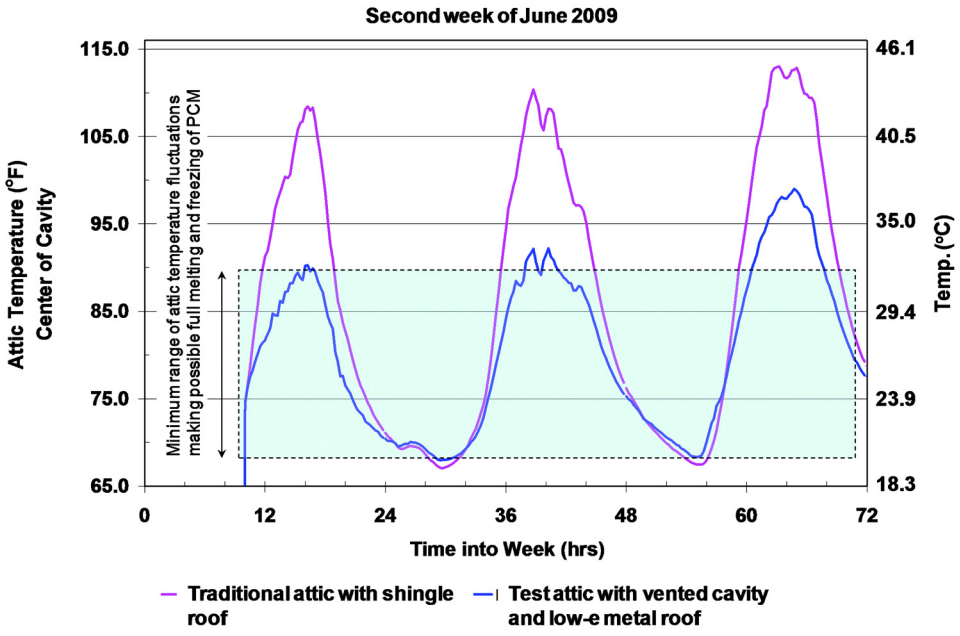

Figure 14 *Attic air temperatures recorded for two experimental attics in June 2009.*

In this experiment, a roof-over-the-roof concept was used in order to add more durable roof surface materials and maximize preservation of the existing roofing components. It is anticipated, that in retrofit applications, this technology may improve overall building envelope energy performance without generating solid waste (very common in reroofing projects). According to California Department of Resources Recycling and Recovery (CalRecycle), approximately 11 million tons (10 million metric tons) of waste in the form of asphalt roofing shingles are generated in the US each year (CalRecycle 2006). It is good to realize that each of listed above elements of roof retrofit could be used independently. PCM together with other novel components is only one of enabling technologies. However, in order to maximize energy savings, all these technologies were integrated together and used at the same time.

During eight weeks of August and September 2008, energy performances of two test attics were monitored and compared. It was found that retrofitted PCM attic with low-e metal roof demonstrated on average an 82% reduction of overall cooling loads in comparison to the traditional R_{SI}-1.2 (R-7) attic with a conventional shingle roof. In order to estimate potential impact of PCM, finite-difference models were developed for the R_{SI}-8.8 (R-50) attic containing PCM-enhanced insulation and for the R_{SI}-8.8 (R-50) attic containing conventional fiberglass insulation as described in (Kosny et al. 2010). Transient simulations were performed for one summer week using experimental data recorded during summer 2006. Numerical analysis of heat fluxes showed about 30% lower overall cooling loads in the case of the attic containing PCM-enhanced insulation.

Another important finding of this research was the fact that the double roof-over-the-roof design is by itself very effective in controlling overall cooling loads. As shown in Figure 14, it was found that during the summer months, the maximum attic temperature in an attic with a double roof (see Figure 4) was about 11°C (20°F) lower than air temperature in a conventional attic with a shingle roof. At the same time, minimum summer attic air temperatures were almost the same. This fact means that, with almost the same attic overnight cooling potential, the conventional shingle roof generates significantly higher thermal loads. However, the observed reduction of the maximum attic air temperature also affects the amplitude of daily temperature fluctuations. In the case of the PCM application, it is critical to select the phase-change temperatures based on expected potential fluctuations of the attic air temperatures, or move the PCM to a different location within the attic. In addition, it is possible to change the amount of PCM. However, it is good to remember that in cases where PCM is not optimized, more PCM (associated with higher cost) may be necessary in order to generate the same energy savings effect.

A design of the attic described in this part of the paper was optimized for cooling-dominated climates. In the northern United States, a shingle roof surface combined with a different location of a PCM heat sink can be used as a passive solar absorber, reducing heating loads during the late fall and early spring months.

CONCLUSIONS

The paper presented experimental and numerical results from thermal performance studies of wall and attic applications of the blown fiberglass insulation modified with a novel spray-applied microencapsulated PCM. Experimental results were reported for both laboratory-scale and full-sized building elements tested in the field. In order to confirm theoretical predictions, it is necessary to remember that wall and attic designs used in this study were optimized for cooling-dominated climates. In the northern United States, different material configurations can be more efficient. For example, in residential buildings with a conventional attic, a shingle roof surface combined with different location of PCM can be used as a passive solar absorber, reducing heating loads during the late fall and early spring months.

For wall applications, PCM-enhanced fiberglass insulation was evaluated during the dynamic guarded hot-box test. The test wall contained approximately 20 wt. % PCM. It was estimated that about 13.6 kg (30 lb) of PCM-enhanced fiberglass insulation (containing 0.79 kg/m^3 [0.16 lb/ft^2] of PCM) was used. The PCM melting temperature was about 29°C (84°F). The phase-change enthalpy was about 170 J/g (73 Btu/lb). Comparisons of measured heat flow rates on the wall surface opposite to the thermal excitation enabled estimation of the potential thermal load reduction generated by the PCM. On average, the PCM part of the wall demonstrated over 27% of the cooling effect (total reduction of the heat flow) during 8 1/2 hours, and over 50% during the first 2 hours of the rapid heating process.

Whole-house energy modeling and full-scale field testing were performed in order to evaluate potential benefits of using PCM-enhanced fiberglass insulation for attic thermal retrofits. Full-scale field testing of residential attics using blown fiberglass and PCM was completed in Oak Ridge, TN. Experimental work was followed by detailed whole-building EnergyPlus simulations in order to generate energy performance data for different US climates. In addition, a series of numerical simulations and field experiments demonstrated a potential for application of a novel PCM-fiberglass insulation as an enabling technology to be used during attic thermal renovations. Five cases of conventional attic insulation were compared against R_{SI}-6.7 (R-38) PCM-enhanced fiberglass. Simulation results for both climates demonstrated a potential for reduction of about 70% to 80% of roof-generated peak-hour loads in the case when conventional R_{SI}-2.1 (R-12) attic insulation was replaced by the R_{SI}-6.7 (R-38) PCM-enhanced fiberglass. Simulation results showed that an upgrade from the conventional R_{SI}-2.1 (R-12) insulation to PCM-enhanced R_{SI}-6.7 (R-38) is 1/3 more energy effective than just using conventional insulation of the same R-value. Similarly, an upgrade from the conventional R_{SI}-3.3 (R-19) insulation to PCM-enhanced R_{SI}-6.7 (R-38) improved overall efficiency by more than 50%.

During eight weeks of August and September 2008, energy performances of two test attics were monitored and compared. It was found that retrofitted PCM attic with a low-e metal roof demonstrated on average an 82% reduction of overall cooling loads in comparison to the traditional R_{SI}-1.2 (R-7) attic with a conventional shingle roof.

REFERENCES

CalRecycle. 2006. Asphalt Roofing Shingles Recycling: Introduction. Construction and Demolition Recycling Web page, www.calrecycle.ca.gov/condemo/Shingles/. Sacramento, CA: California Department of Resources Recycling and Recovery.

Kosny, J. 2008. *2006/07 field testing of cellulose fiber insulation enhanced with phase change material*. Report ORNL/TM-2007/186, Oak Ridge, TN: Oak Ridge National Laboratory.

Kosny, J., D. Yarbrough, and K. Wilkes. 2006. *PCM-enhanced cellulose insulation: Thermal mass in lightweight fibers*. Presented at International Energy Agency and Department of Energy Ecostock 2006 Conference.

Kosny, J., D. Yarbrough, T.W. Petrie, and A. Syed. 2007a. *Performance of thermal insulation containing microencapsulated phase change material*. Presented at 2007 International Thermal Conductivity Conference.

Kosny, J., D. Yarbrough, W. Miller, T. Petrie, P. Childs, and A. Syed. 2007b. *Thermal performance of PCM-enhanced building envelope systems*. Presented at Thermal Envelopes X Conference.

Kosny, J., D.W. Yarbrough, W.A. Miller, K.E. Wilkes, and E.S. Lee. 2009. *Analysis of the dynamic thermal performance of fibrous insulations containing phase change materials*. Presented at 11th International Conference on Thermal Energy Storage, Effstock 2009, Thermal Energy Storage for Energy Efficiency and Sustainability, Stockholm.

Kosny, J., W. Miller, and A. Zaltash. 2010. *Dynamic thermally-disconnected building envelopes—A new paradigm for walls and roofs in zero energy buildings*. Thermal Envelopes XI Conference.

Kossecka, E. 1998. Relationships between structure factors, response factors and *Z*-transfer function coefficients for multilayer walls. *ASHRAE Transactions* 104(1):68–77.

Kossecka, E. and J. Kosny. 2002. Influence of insulation configuration on heating and cooling loads in a continuously used building. *Energy & Buildings* 34(4):321–331.

Kossecka, E. and J. Kosny. 2008. Hot box testing of building envelope assemblies: A simplified procedure for estimation of minimum time of the test. *Journal of Testing and Evaluation* 36(3):242–249.

Kossecka, E. and J. Kosny 2009. Dynamiczna Metoda Pomiaru Zawartosci Materialu Fazowo Zmiennego w Izolacji. *Proceedings of the XII Conference Building Physics in Theory and Practice*, Lodz University, Poland.

Miller, W.A. and J. Kosny. 2007. Next-generation roofs and attics for residential homes. *Proceedings of the 2007 ACEEE Summer Studies on Energy Efficiency.*

Petrie, T.W., K.W. Childs, P.W. Childs, J.E. Christian, and D.J. Shramo. 1997. Thermal behavior of mixtures of perlite and phase change material in a simulated climate. *ASTM STP 1320: Insulation Materials: Testing and Applications*, 3rd vol., pp. 180–194, R.S. Graves and R.R. Zarr, eds. West Conshohocken, PA: American Society for Testing and Materials.

Tomlinson, J., C. Jotshi, and D. Goswami. 1992. Solar thermal energy storage in phase change materials. *Proceedings of Solar '92: The American Solar Energy Society Annual Conference*, pp. 174–79.